# UPDATED CPUE STANDARDIZATION FOR SWORDFISH (XIPHIAS GLADIUS) IN THE INDIAN OCEAN USING A ZERO-INFLATED BAYESIAN HIERARCHICAL SPATIAL MODEL WITH JAPANESE LONGLINE FISHERY DATA (1994-2024)

Shoma Takahashi[1]*, Takayuki Matsumoto[1], and Mikihiko Kai[1]
*takahashi_shoma84@fra.go.jp

[1] *Fisheries Resources Institute, Japan Fisheries Research and Education Agency, 2-12-4, Fukuura, Kanazawa-ku, Yokohama-shi, 236-8648, Japan*

**Abstract**

CPUE standardization of swordfish (1994-2024) in the Indian Ocean was conducted using data from four areas (NW, NE, SW, and SE) collected by Japanese longliners. We applied Bayesian hierarchical spatial models to standardize the CPUE. Since the catch data contained many zero observations, we used zero-inflated Poisson generalized linear mixed model (ZIP-GLMM). To ensure consistency with

the previous stock assessment, the model structures adopted in Matsumoto et al. (2023) were retained and applied to the updated dataset without modification. The standardized CPUE trends were generally similar among areas, although some differences were evident. The standardized CPUE declined from the mid-1990s to the early 2000s in all areas, whereas subsequent trends differed among areas. Comparison with previous studies indicated that the temporal trends in standardized CPUE were generally consistent among studies for each area.

## 1. Introduction

Hierarchical Bayesian models have traditionally relied on Markov chain Monte Carlo (MCMC) methods, which are computationally intensive and technically, thereby limiting widespread application. However, a statistical approach, namely Integrated Nested Laplace Approximations (INLA), is now readily available through the R-INLA package (http://www.rhttp://www.r-inla.org/inla.org). The INLA methodology and its powerful application for modelling complex datasets have recently been introduced to a wider nontechnical audience (Illian et al. 2013). Unlike MCMC methods, INLA uses deterministic approximation for statistical inference, thereby avoiding the substantial computational burden as well as the convergence and mixing problems that are sometimes encountered with MCMC algorithms (Rue and Martino 2007). Moreover, the stochastic partial differential equations (SPDE) approach (Lindgren et al. 2011), implemented in R-INLA, represents another important statistical development. It enables much faster modeling of spatial random effect represented as Gaussian random field (GRFs) and provides a flexible framework for handling datasets with complex spatial structure (Lindgren and Rue 2015). This is often the case for fisheries data, as fishers frequently shift their fishing grounds, resulting in clustered spatial patterns and large areas with little or no data. Together, these advances in statistical methodology and their implementation in R allow scientists to fit complex spatiotemporal models more rapidly and reliably (Rue et al. 2009, Cosandey-Godin et al. 2015).

The aim of this study is to update the historical trajectory of the swordfish (*Xiphias gladius*) abundance index in the Indian Ocean based on catches by Japanese longliners during 1994-2024, for the four areas (Northwest: NW, Northeast: NE , Southwest: SW, and Southeast: SE) used in the last stock assessment, using zero-inflated Bayesian hierarchical spatial models fitted with INLA and SPDE approach.

## 2. Materials and methods

### Data sets

Japanese longline logbook data (set-by-set data) was used for the CPUE standardization of the swordfish in the Indian Ocean. The format of the Japanese logbook was revised in 1994, and the fishing practices affecting catchability ($q$), such as the materials used for mainlines and branch lines and gear configuration (e.g., number of hooks per basket), also changed during the mid-1990s. Because detailed information on this change is not fully available in the logbook data, only data collected from 1994 onward were used in the analysis. The spatial and temporal resolutions of the logbook were 1° × 1° grid cells and one day, respectively. For consistency with previous assessment, we adopted the same four analysis areas (NW, NE, SW, and SE) established for swordfish CPUE standardization by the 9th Session of the IOTC Working Party on Billfish (IOTC 2014; **Fig. 1**).

### Statistical models

In this analysis, we applied Bayesian hierarchical spatial models. We did not consider spatiotemporal models because they are computationally demanding, and previous analysis showed only small differences in the Widely Applicable Bayesian Information Criterion (WAIC; Watanabe, 2013) between spatial and spatiotemporal models (Taki et al., 2020). Since the catch data contained a high proportion of zero catches (**Fig. 2**), we evaluated a zero-inflated Poisson generalized linear mixed model (ZIP-GLMM). Zero-inflated model is particularly useful for fisheries data because they explicitly account for excess zeros and distinguish between structural and sampling zeros. An alternative approach for handling excess zeros is the zero-inflated negative binomial generalized linear mixed model (ZINB-GLMM). However, the ZINB may result in underdispersion in some applications (e.g., Ijima 2017). Therefore, we considered the ZIP-GLMM to be more appropriate for CPUE standardization in this study.

For the explanatory variables, year (yr) and quarter (Jan-Mar, Apr-Jun, Jul-Sep, Oct-Dec; qtr) were included as fixed effect, whereas area represented by 5° × 5° spatial cells (latlon), gear configuration represented by the number of hooks per basket (hpb), and vessel identity represented by vessel name (jp_name) were included as random effects. The number of hpb generally increased until the mid-1990s (**Fig. 3**). Most variables were treated as categorical factors, however, for some spatial models, year was modeled as a first-order autoregressive process (AR1) to account for temporal dependence and reduce uncertainty in annual estimates. The inclusion of random effects was appropriate because vessel identity, gear configuration, and 5° × 5° spatial cells each contained a large number of levels. The random effect model also helped account for pseudo-replication associated with vessel identity, gear configuration, and operating area.

All analyses were conducted in R using the R-INLA package. Consistent with the Bayesian framework, INLA estimates the marginal posterior distributions of all parameters and random effects. A half Cauchy prior was specified for the random effect variance parameters. The model structure adopted in the previous stock assessment (Matsumoto et al., 2023) was applied to the updated dataset.

## 3. Results and discussions

### Overview of catch and effort

The distribution of fishing effort by Japanese longline fishery is shown in **Fig. 4** for the entire study period, **Fig. 5** by decade, and **Fig. 6** annually from 1994 onward. Fishing effort was distributed throughout most of the Indian Ocean, although little or no effort occurred in the central southern region (**Fig. 4**). In recent years, particularly since the 2010s, the distribution of fishing effort has become more spatially concentrated (**Fig. 5**). Since the late 2000s, fishing effort in the southeastern Indian Ocean has been concentrated in the eastern sector (off the west coast of Australia), reflecting an overall reduction in total fishing efforts. Fishing effort in the northwestern Indian Ocean has also declined markedly since 2015 (**Fig. 6**).

**Fig. 7** shows the distribution of nominal CPUE (number of fish per 1000 hooks) for swordfish caught by the Japanese longline fishery in the Indian Ocean, averaged over 1994-2024. In general, CPUE was higher in tropical waters, particularly in the western Indian Ocean. Relatively high CPUE values were also observed in the southeastern Indian Ocean, especially off the **W**estcoast of Australia.

**Fig. 8** shows the mean body weight (kg) of swordfish caught by the Japanese longline fishery in the Indian Ocean, averaged over 1994-2024. Mean body weight was generally higher in temperate waters than in tropical waters. Within the temperate region between 30 °S and 40 °S, mean body weight was higher in the western area (west of 80° E) than in the eastern area (east of 80° E).

### Standardized CPUE

The four models (one for each area) adopted in the previous stock assessment (Matsumoto et al., 2023) were applied to the updated dataset without modification and, no model selection was conducted using the WAIC (**Table 1**). The previous model structure was retained to ensure consistency with the earlier assessment, as the CPUE index for the northwestern area has already been incorporated into the management strategy evaluation (MSE).

**Northwest**

The posterior distributions are shown in **Fig. 9**, and the estimated marginal distributions appeared reasonable. The mean latent spatial field indicated that the southeastern region had a negative effect on standardized CPUE during 1994-2024, whereas the western coastal region had a positive effect on standardized CPUE throughout the study period (**Fig. 10**). Annual estimated CPUE showed a declining trend during the 1990s and the beginning of the 2000s, followed by a slightly increasing trend from 2006 onward (**Fig. 11, Table 2**).

**Northeast**

The posterior distributions are shown in **Fig. 12**, and the estimated marginal distributions appeared reasonable. The offshore area of the western Indian Ocean, particularly south of India, exhibited a consistently positively correlated with the swordfish CPUE throughout the study period (**Fig. 13**). No apparent trend was observed in the interannual variation of standardized CPUE (**Fig. 14**, **Table 3**).

**Southwest**

The posterior distributions are shown in **Fig. 15**, and the estimated marginal distributions appeared reasonable. The western coastal region exhibited a consistently positive spatial effect on swordfish CPUE throughout the study period (**Fig. 16**). Annual estimated CPUE showed a declining trend during the 1990s, followed by an increasing trend from 2004 onward (**Fig. 17**, **Table 4**).

**Southeast**

The posterior distributions are shown in **Fig. 18**, and the estimated marginal distributions appeared reasonable. No apparent trend was observed in interannual variation of standardized CPUE (**Fig. 19**, **Table 5**).

**Fig. 20** compares the relative CPUE among areas. Overall, temporal trends were similar among areas, although some differences were evident. For example, CPUE declined from the mid-1990s to the early 2000s in all areas. Thereafter, increasing trends were observed until the late 2010s in all areas except the southeastern area. However, the subsequent trends differed among areas.

**Comparison with CPUE in the previous study and nominal CPUE**

**Fig. 21** compares the standardized CPUE estimates from the present study with those from previous studies that used similar methods (Taki et al., 2020; Matsumoto et al., 2023;  IOTC 2024 [Northwest area only]), as well as with nominal CPUE. For each area, the temporal trends in the point estimates of standardized CPUE were generally consistent among studies. The trends in standardized CPUE were also broadly consistent with those in nominal CPUE, except in the southeastern area, where the nominal CPUE showed a substantial increase in the early 2010s. The reason for the discrepancy between the nominal CPUE and the model-estimated standardized CPUE in the southeastern area remains unclear. Preliminary analyses indicate that the discrepancy may be attributable to limitations of the model itself.

## 4. References

Cosandey-Godin, A., Krainski, E. T., Worm, B. and Flemming, J. M. 2015. Applying Bayesian spatiotemporal models to fisheries bycatch in the Canadian Arctic. Can. J. Fish. Aquat. Sci. 72: 186–197. dx.doi.org/10.1139/cjfas-2014-0159.

Ijima, H. 2017. CPUE standardization of the Indian Ocean swordfish (*Xiphias gladius*) by Japanese longline fisheries: Using negative binomial GLMM and zero inflated negative binomial GLMM to consider vessel effect. IOTC-2017-WPB15-19.

Illian, J.B., Martino, S., Sørbye, S.H., Gallego-Fernández, J.B., Zunzunegui, M., Paz Esquivias, M., and Travis, J.M.J. 2013. Fitting complex ecological point process models with integrated nested Laplace approximation. Methods Ecol. Evol. 4(4): 305–315. doi:10.1111/2041210x.12017.

IOTC. 2014. Report of the 12th session of the IOTC working party on billfish. IOTC-2014-WPB-R [E].

IOTC. 2024. Standardized CPUE data for Swordfish. IOTC-2024-WPB22-DATA12. https://iotc.org/WPB/22/Data/12-CPUEDataSWO.

Lindgren, F., and Rue, H. 2015. Bayesian Spatial Modelling with R-INLA. Journal of Statistical Software 63(19): 1–25. doi:10.18637/jss.v063.i19.

Lindgren, F., Rue, H., and Lindström, J. 2011. An explicit link between Gaussian fields and Gaussian Markov random fields: the stochastic partial differential equation approach. J. R. Stat. Soc. Ser. B Stat. Methodol. 73(4): 423–498. doi:10.1111/j.1467-9868.2011.00777.x.

Matsumoto, T., Taki, K., Ijima, H. and Kai, M. 2023. CPUE standardization for swordfish (*Xiphias gladius*) by Japanese longline fishery in the Indian Ocean using zero-inflated Bayesian hierarchical spatial model. IOTC-2023-WPB21-14_Rev1.

Rue, H., and Martino, S. 2007. Approximate Bayesian inference for hierarchical Gaussian Markov random field models. J. Stat. Plann. Infer. 137(10): 3177–3192. doi:10.1016/j.jspi.2006.07.016.

Rue, H., Martino, S., and Chopin, N. 2009. Approximate Bayesian inference for latent Gaussian models by using integrated nested Laplace approximations. J. R. Stat. Soc. Ser. B Stat. Methodol. 71(2): 319–392. doi:10.1111/j.1467-9868. 2008.00700.x.

Taki, K., Ijima, H. and Y. Semba. 2020. Japanese Longline CPUE Standardization (1979-2018) for Swordfish (*Xiphias gladius*) in the Indian Ocean using zero-inflated Bayesian hierarchical spatial model. IOTC-2020-WPEB18-14.

Watanabe, S. 2013. A widely applicable Bayesian information criterion. Journal of Machine Learning Research 14: 867-897.

**Table 1.** Specification of the two model types and four analysis areas adopted in the previous stock assessment (Matsumoto et al., 2023) ,and also used in this study.

| Model | Area |
|---|---|
| m_zip_spde2 =inla(swo ~ 0 + intercept + f(year, model = "ar1") + f(month, model = "iid", hyper=hcprior) + f(w, model=spde) + f(hpb, model="iid", hyper=hcprior) + f(jp_name, model="iid", hyper=hcprior),<br>data = inla.stack.data(StackFit_m) , offset = log(d$hooks/1000), family = "zeroinflatedpoisson1") | NW<br>NE<br>SW |
| m_zip_glmm= inla(swo ~ yr + qtr + f(latlon, model = "iid") + f(jp_name, model = "iid"),<br>data=d,offset=log(d$hooks/1000), family="zeroinflatedpoisson1")) | SE |

**Table 2.** Nominal and standardized CPUEs in the **northwestern** Indian Ocean during 1994-2024, with 95% confidence intervals.

| Year | Nominal | Standardized | 2.5% | 97.5% |
|---|---|---|---|---|
| 1994 | 0.95 | 0.92 | 0.77 | 1.10 |
| 1995 | 0.78 | 0.70 | 0.58 | 0.83 |
| 1996 | 0.70 | 0.58 | 0.49 | 0.70 |
| 1997 | 0.73 | 0.58 | 0.48 | 0.69 |
| 1998 | 0.71 | 0.60 | 0.50 | 0.72 |
| 1999 | 0.49 | 0.45 | 0.38 | 0.54 |
| 2000 | 0.50 | 0.44 | 0.36 | 0.52 |
| 2001 | 0.61 | 0.55 | 0.46 | 0.66 |
| 2002 | 0.52 | 0.51 | 0.42 | 0.60 |
| 2003 | 0.43 | 0.39 | 0.32 | 0.46 |
| 2004 | 0.39 | 0.34 | 0.28 | 0.40 |
| 2005 | 0.40 | 0.33 | 0.28 | 0.40 |
| 2006 | 0.41 | 0.30 | 0.25 | 0.36 |
| 2007 | 0.52 | 0.38 | 0.32 | 0.45 |
| 2008 | 0.46 | 0.34 | 0.29 | 0.41 |
| 2009 | 0.45 | 0.39 | 0.33 | 0.47 |
| 2010 | 0.46 | 0.47 | 0.39 | 0.56 |
| 2011 | NA | 0.48 | 0.32 | 0.71 |
| 2012 | 0.79 | 0.48 | 0.39 | 0.61 |
| 2013 | 0.60 | 0.34 | 0.27 | 0.42 |
| 2014 | 0.34 | 0.31 | 0.25 | 0.38 |
| 2015 | 0.64 | 0.58 | 0.47 | 0.71 |
| 2016 | 0.73 | 0.60 | 0.48 | 0.74 |
| 2017 | 0.89 | 0.71 | 0.58 | 0.87 |
| 2018 | 0.59 | 0.43 | 0.35 | 0.54 |
| 2019 | 0.42 | 0.45 | 0.35 | 0.57 |
| 2020 | 0.41 | 0.41 | 0.32 | 0.53 |
| 2021 | 0.42 | 0.45 | 0.34 | 0.60 |
| 2022 | 0.55 | 0.53 | 0.41 | 0.68 |
| 2023 | 0.67 | 0.45 | 0.36 | 0.55 |
| 2024 | NA | 0.46 | 0.29 | 0.73 |

**Table 3.** Nominal and standardized CPUEs in the **northeastern** Indian Ocean during 1994-2024, with 95% confidence intervals.

| Year | Nominal | Standardized | 2.5% | 97.5% |
|---|---|---|---|---|
| 1994 | 0.39 | 0.30 | 0.07 | 1.21 |
| 1995 | 0.36 | 0.27 | 0.06 | 1.09 |
| 1996 | 0.42 | 0.30 | 0.07 | 1.23 |
| 1997 | 0.47 | 0.32 | 0.08 | 1.30 |
| 1998 | 0.42 | 0.28 | 0.07 | 1.13 |
| 1999 | 0.38 | 0.27 | 0.06 | 1.09 |
| 2000 | 0.32 | 0.20 | 0.05 | 0.82 |
| 2001 | 0.25 | 0.17 | 0.04 | 0.71 |
| 2002 | 0.21 | 0.16 | 0.04 | 0.65 |
| 2003 | 0.27 | 0.20 | 0.05 | 0.82 |
| 2004 | 0.20 | 0.15 | 0.03 | 0.60 |
| 2005 | 0.24 | 0.17 | 0.04 | 0.71 |
| 2006 | 0.24 | 0.15 | 0.03 | 0.59 |
| 2007 | 0.35 | 0.19 | 0.04 | 0.76 |
| 2008 | 0.40 | 0.17 | 0.04 | 0.71 |
| 2009 | 0.32 | 0.18 | 0.04 | 0.74 |
| 2010 | 0.28 | 0.18 | 0.04 | 0.74 |
| 2011 | 0.27 | 0.17 | 0.04 | 0.70 |
| 2012 | 0.26 | 0.17 | 0.04 | 0.70 |
| 2013 | 0.36 | 0.20 | 0.05 | 0.84 |
| 2014 | 0.51 | 0.27 | 0.06 | 1.11 |
| 2015 | 0.54 | 0.28 | 0.07 | 1.15 |
| 2016 | 0.69 | 0.38 | 0.09 | 1.55 |
| 2017 | 0.50 | 0.28 | 0.07 | 1.13 |
| 2018 | 0.55 | 0.29 | 0.07 | 1.18 |
| 2019 | 0.58 | 0.31 | 0.07 | 1.26 |
| 2020 | 0.68 | 0.35 | 0.08 | 1.44 |
| 2021 | 0.61 | 0.32 | 0.08 | 1.31 |
| 2022 | 0.57 | 0.31 | 0.07 | 1.28 |
| 2023 | 0.48 | 0.29 | 0.07 | 1.17 |
| 2024 | 0.63 | 0.34 | 0.08 | 1.38 |

**Table 4.** Nominal and standardized CPUEs in the **southwestern** Indian Ocean during 1994-2024, with 95% confidence intervals.

| Year | Nominal | Standardized | 2.5% | 97.5% |
|---|---|---|---|---|
| 1994 | 0.41 | 1.14 | 0.88 | 1.49 |
| 1995 | 0.27 | 0.78 | 0.60 | 1.03 |
| 1996 | 0.27 | 0.75 | 0.58 | 0.99 |
| 1997 | 0.30 | 0.73 | 0.56 | 0.96 |
| 1998 | 0.23 | 0.55 | 0.42 | 0.71 |
| 1999 | 0.19 | 0.44 | 0.34 | 0.57 |
| 2000 | 0.21 | 0.40 | 0.31 | 0.53 |
| 2001 | 0.17 | 0.35 | 0.27 | 0.46 |
| 2002 | 0.16 | 0.36 | 0.27 | 0.46 |
| 2003 | 0.12 | 0.30 | 0.23 | 0.39 |
| 2004 | 0.17 | 0.39 | 0.30 | 0.51 |
| 2005 | 0.20 | 0.42 | 0.32 | 0.55 |
| 2006 | 0.26 | 0.47 | 0.36 | 0.62 |
| 2007 | 0.23 | 0.36 | 0.28 | 0.47 |
| 2008 | 0.29 | 0.44 | 0.34 | 0.58 |
| 2009 | 0.40 | 0.63 | 0.48 | 0.82 |
| 2010 | 0.33 | 0.60 | 0.46 | 0.78 |
| 2011 | 0.38 | 0.61 | 0.47 | 0.80 |
| 2012 | 0.32 | 0.53 | 0.41 | 0.69 |
| 2013 | 0.29 | 0.48 | 0.37 | 0.63 |
| 2014 | 0.27 | 0.42 | 0.32 | 0.56 |
| 2015 | 0.28 | 0.47 | 0.36 | 0.61 |
| 2016 | 0.43 | 0.67 | 0.51 | 0.88 |
| 2017 | 0.48 | 0.70 | 0.54 | 0.92 |
| 2018 | 0.38 | 0.63 | 0.48 | 0.83 |
| 2019 | 0.37 | 0.65 | 0.49 | 0.85 |
| 2020 | 0.37 | 0.60 | 0.46 | 0.79 |
| 2021 | 0.31 | 0.50 | 0.38 | 0.66 |
| 2022 | 0.47 | 0.64 | 0.48 | 0.84 |
| 2023 | 0.53 | 0.70 | 0.53 | 0.92 |
| 2024 | 0.67 | 0.78 | 0.59 | 1.02 |

**Table 5.** Nominal and standardized CPUEs in the **southeastern** Indian Ocean during 1994-2024, with 95% confidence intervals.

| Year | Nominal | Standardized | 2.5% | 97.5% |
|---|---|---|---|---|
| 1994 | 0.17 | 0.21 | 0.03 | 1.70 |
| 1995 | 0.19 | 0.21 | 0.03 | 1.74 |
| 1996 | 0.27 | 0.23 | 0.03 | 1.86 |
| 1997 | 0.37 | 0.26 | 0.03 | 2.13 |
| 1998 | 0.17 | 0.21 | 0.03 | 1.73 |
| 1999 | 0.25 | 0.24 | 0.03 | 1.95 |
| 2000 | 0.22 | 0.23 | 0.03 | 1.85 |
| 2001 | 0.14 | 0.16 | 0.02 | 1.31 |
| 2002 | 0.17 | 0.19 | 0.02 | 1.52 |
| 2003 | 0.14 | 0.18 | 0.02 | 1.45 |
| 2004 | 0.21 | 0.18 | 0.02 | 1.49 |
| 2005 | 0.10 | 0.12 | 0.02 | 1.00 |
| 2006 | 0.25 | 0.16 | 0.02 | 1.33 |
| 2007 | 0.47 | 0.19 | 0.02 | 1.58 |
| 2008 | 0.31 | 0.17 | 0.02 | 1.35 |
| 2009 | 0.27 | 0.14 | 0.02 | 1.16 |
| 2010 | 0.39 | 0.16 | 0.02 | 1.28 |
| 2011 | 0.48 | 0.18 | 0.02 | 1.50 |
| 2012 | 0.44 | 0.16 | 0.02 | 1.28 |
| 2013 | 0.50 | 0.18 | 0.02 | 1.45 |
| 2014 | 0.51 | 0.19 | 0.02 | 1.55 |
| 2015 | 0.43 | 0.17 | 0.02 | 1.41 |
| 2016 | 0.31 | 0.11 | 0.01 | 0.92 |
| 2017 | 0.28 | 0.11 | 0.01 | 0.87 |
| 2018 | 0.26 | 0.11 | 0.01 | 0.91 |
| 2019 | 0.29 | 0.10 | 0.01 | 0.84 |
| 2020 | 0.33 | 0.16 | 0.02 | 1.29 |
| 2021 | 0.22 | 0.12 | 0.02 | 0.99 |
| 2022 | 0.22 | 0.13 | 0.02 | 1.04 |
| 2023 | 0.15 | 0.16 | 0.02 | 1.29 |
| 2024 | 0.09 | 0.14 | 0.02 | 1.12 |

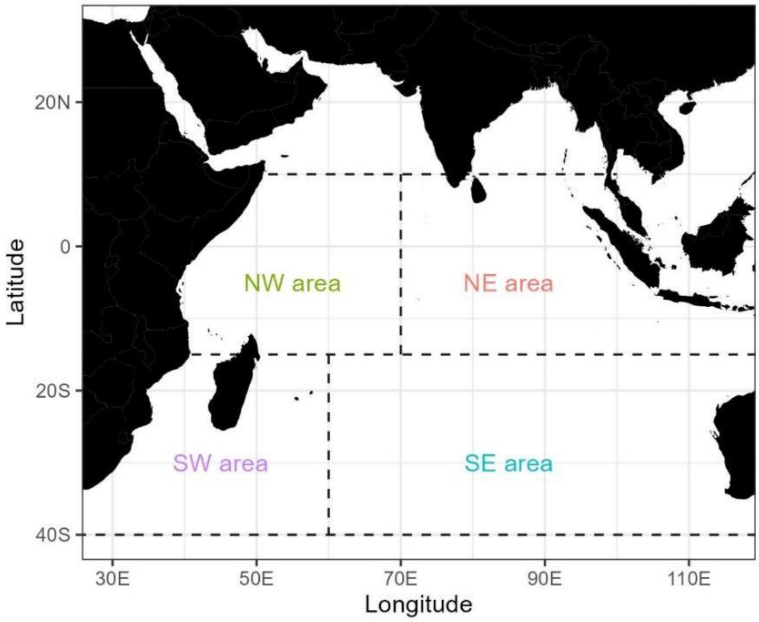


**Fig. 1.** Geographic boundaries of the four analysis areas used for swordfish CPUE standardization in the Indian Ocean.

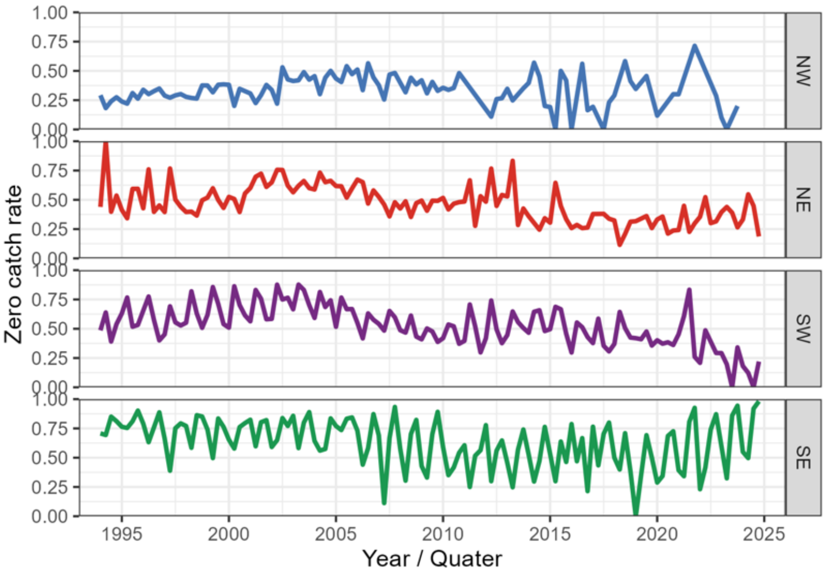


**Fig. 2.** Year-season specific zero catch rate of swordfish in the Japanese longline fishery for each analysis area.

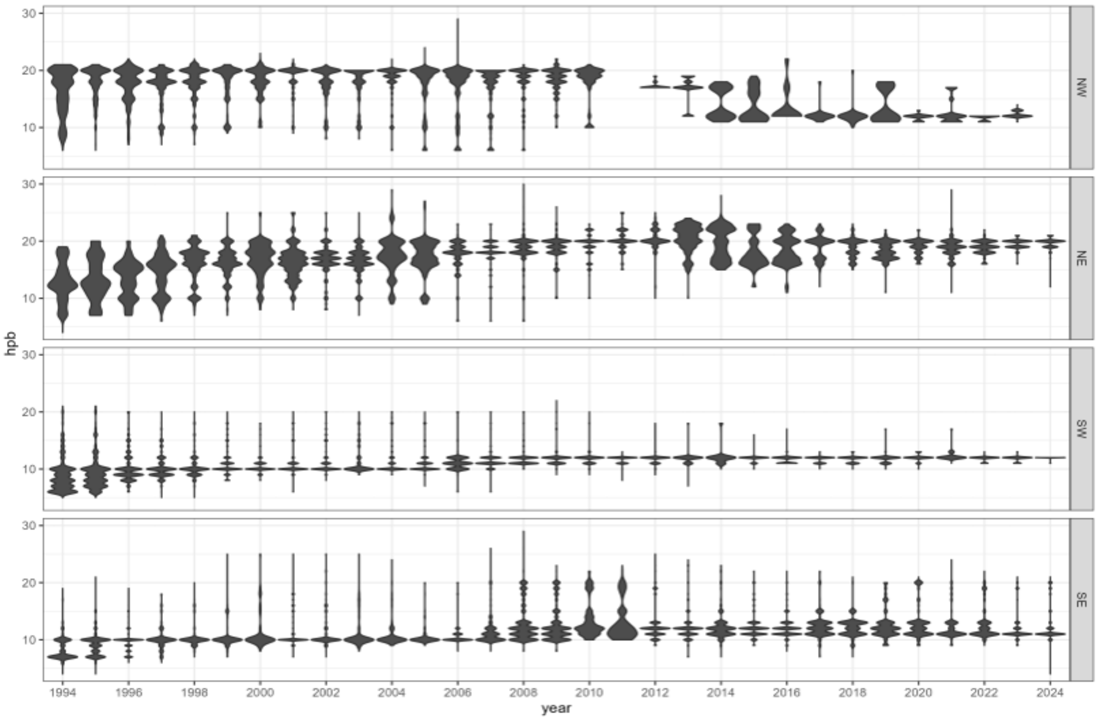


**Fig. 3.** Historical changes in gear setting (number of hooks per basket) in the Japanese longline fishery in the Indian Ocean. Gear configuration differs between the northern and southern Indian Ocean because Japanese longliners commonly targets southern bluefin tuna in the south Indian Ocean. In each violine plot, the vertical extent represents the range of the data, and width indicates the relative frequency of observations.

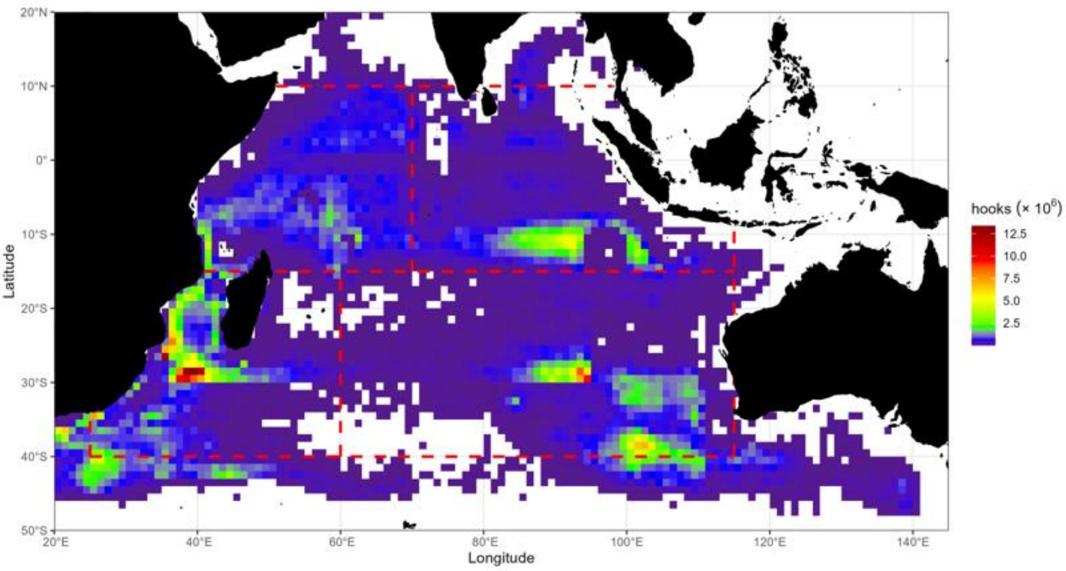

**Fig. 4.** Spatial distribution of fishing effort by the Japanese longline fishery in the Indian Ocean during 1994-2024 and borders of four areas (red broken lines).

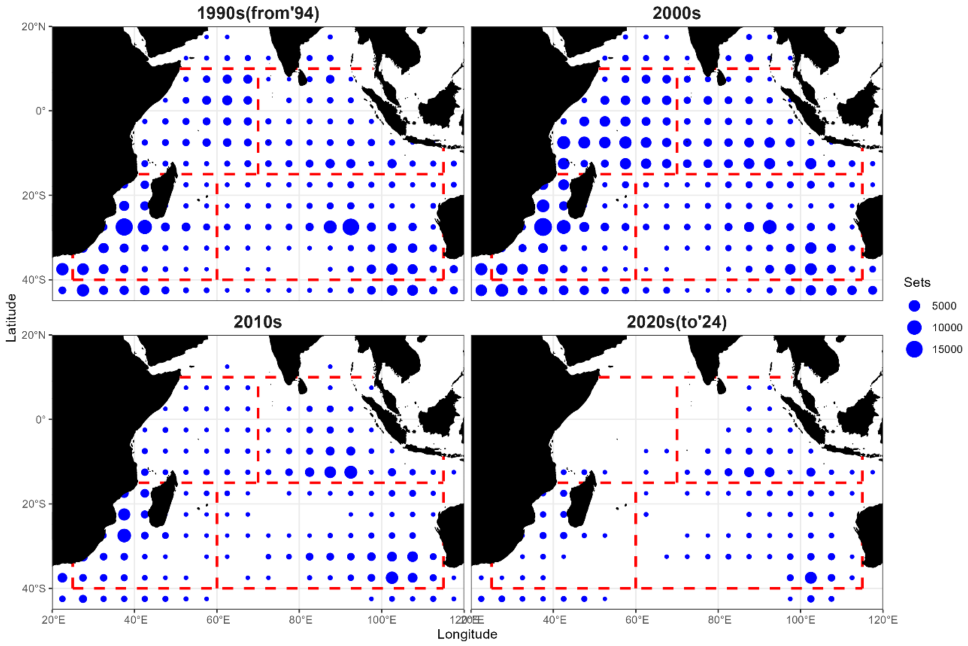


**Fig. 5.** Spatial distribution of fishing effort (number of sets) by the Japanese longline fishery in the Indian Ocean by decade and borders of four areas (red broken lines).

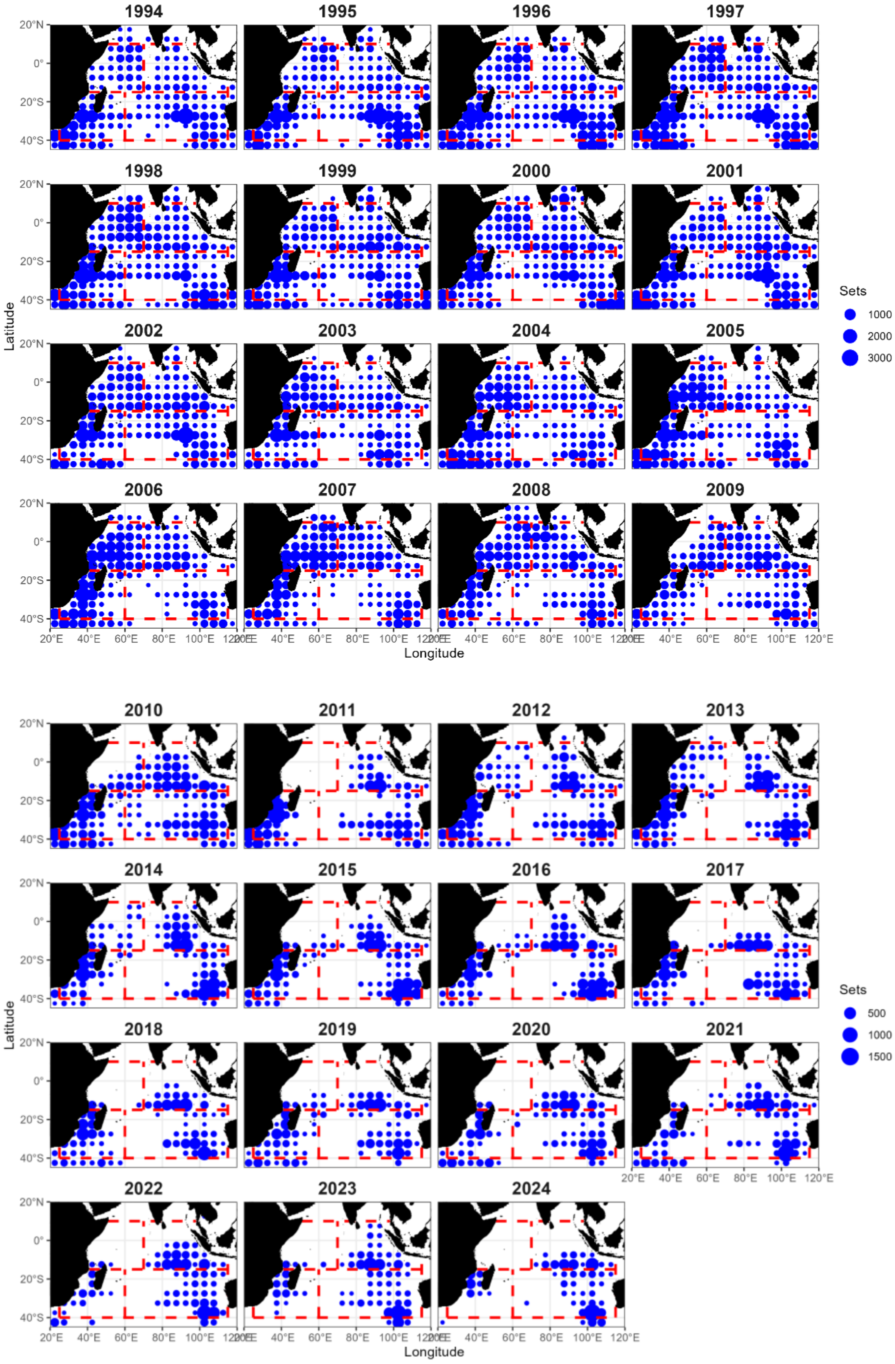


**Fig. 6.** Annual spatial distribution of fishing effort (number of sets) by the Japanese longline fishery in the Indian Ocean from 1994 onward. Dashed lines indicate the boundaries of the areas used for CPUE standardization.

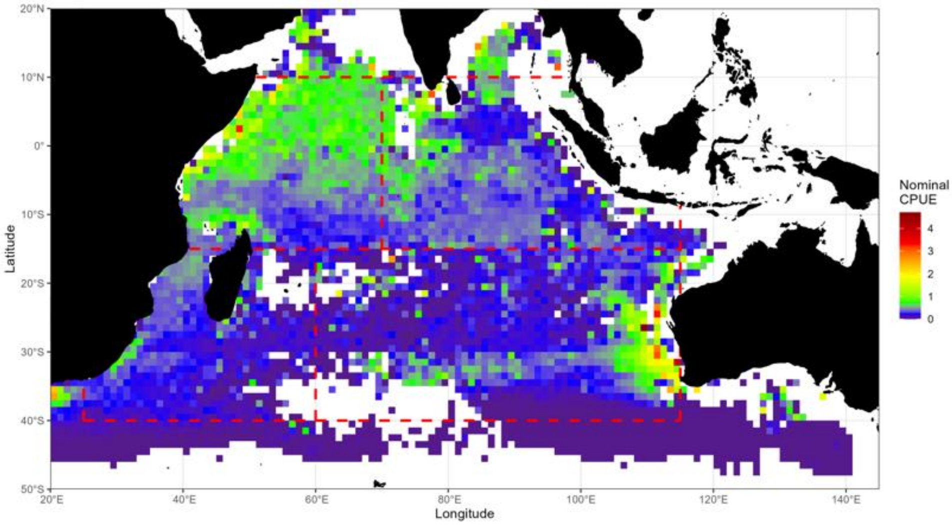


**Fig. 7.** Spatial distribution of nominal swordfish CPUE (number of fish per 1000 hooks) in the Japanese longline fishery in the Indian Ocean, averaged over 1994-2024. Dashed lines indicate the boundaries of the areas used for CPUE standardization.

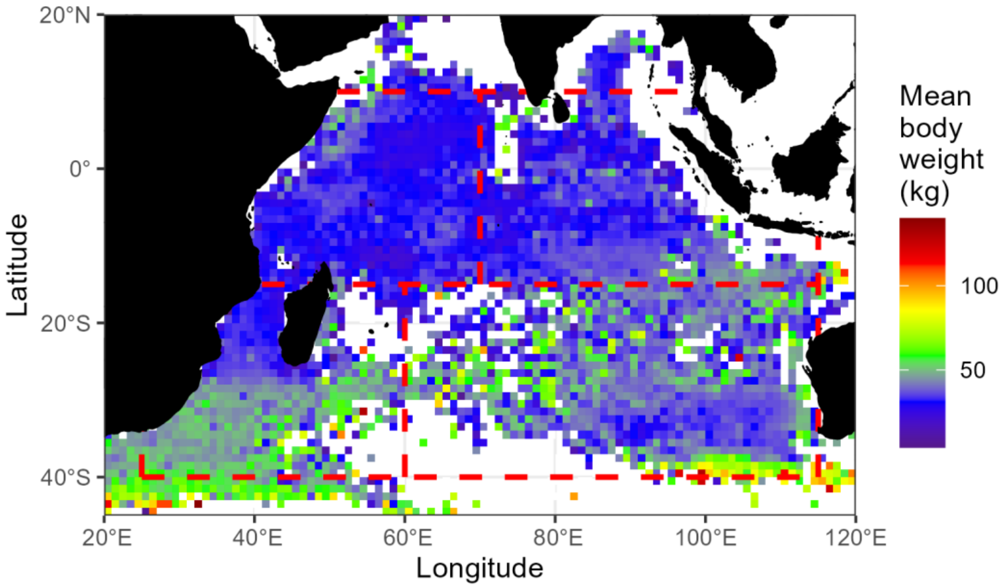


**Fig. 8.** Spatial distribution of the mean body weight (kg) of swordfish in the Japanese longline fishery in the Indian Ocean averaged over 1994-2024.

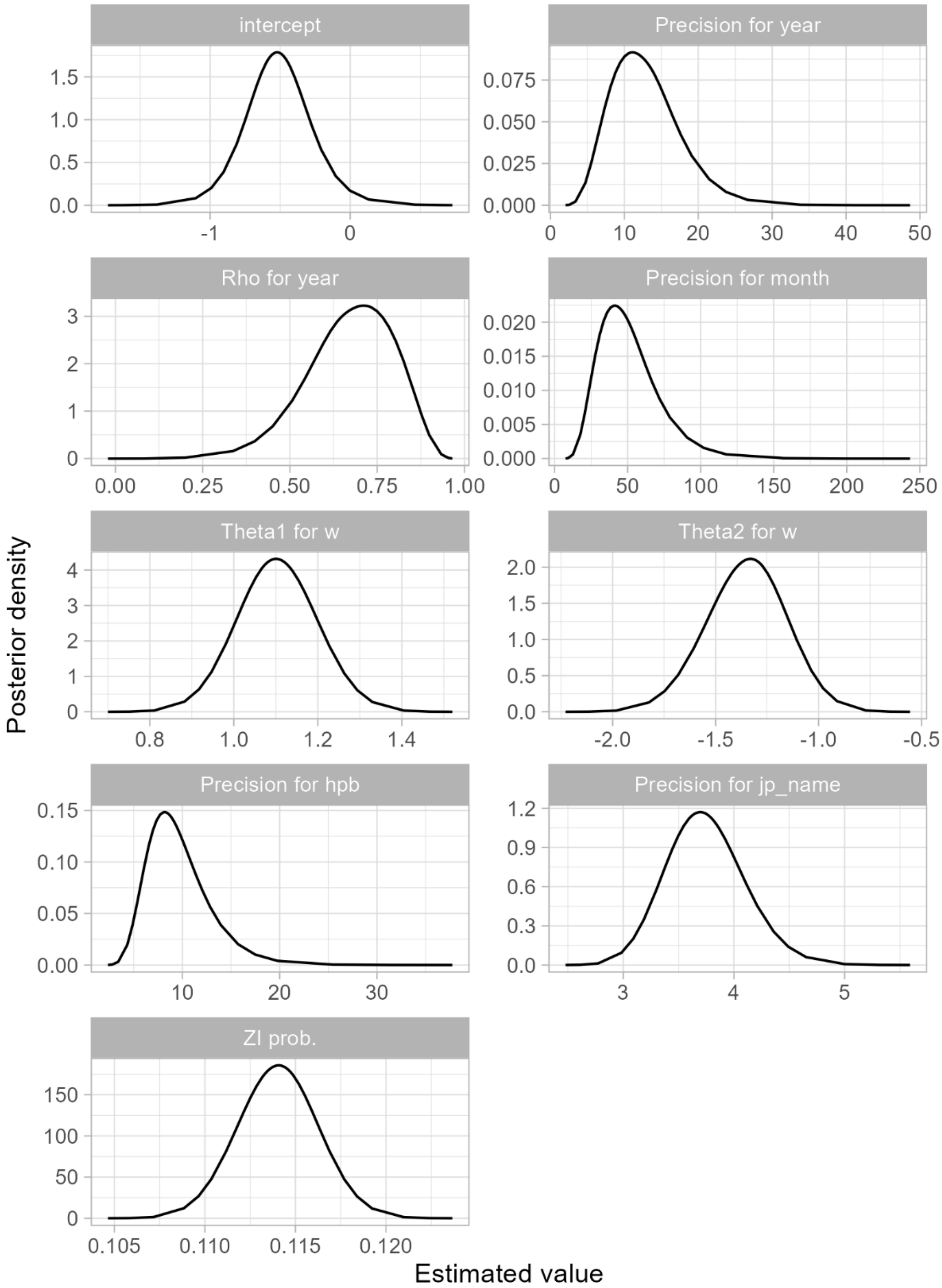


**Fig. 9. Northwest.** Posterior marginal distributions of the fixed effect (intercept), random-effect precision parameters, temporal correlation parameter (Rho), and spatial field parameters (Thetas).

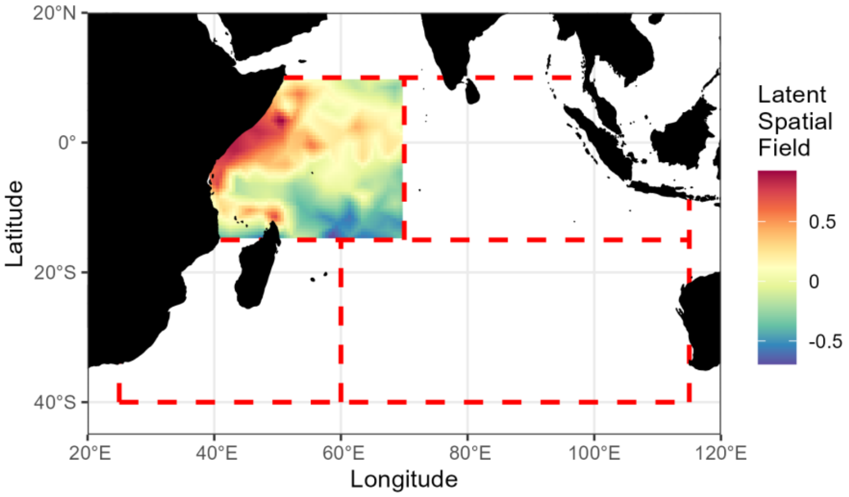


**Fig. 10.** Mean latent spatial field for the northwestern Indian Ocean.

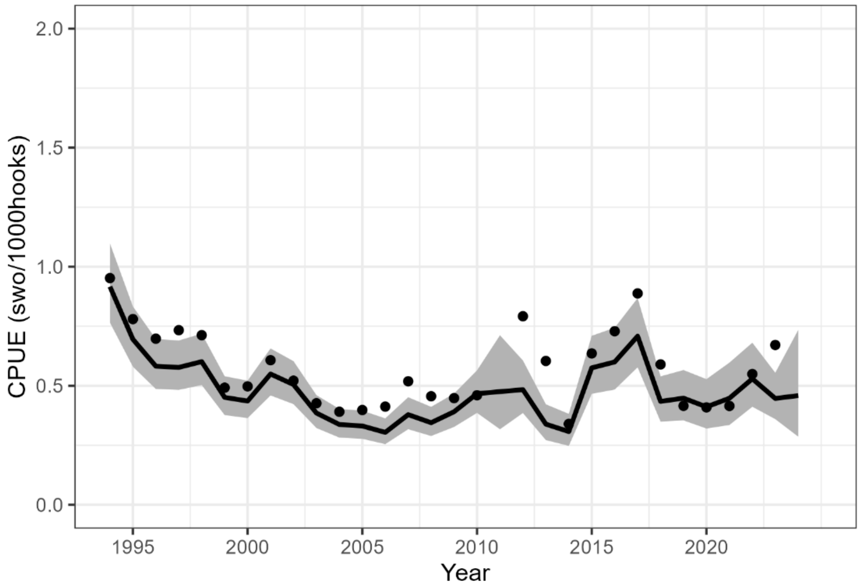


**Fig. 11. Northwestern Indian Ocean.** Historical changes in CPUE. The solid line represents the standardized CPUE (number of swordfish per 1,000 hooks) and the shaded area indicates the 95% credible interval. Points denote nominal CPUE (number of swordfish per 1,000 hooks).

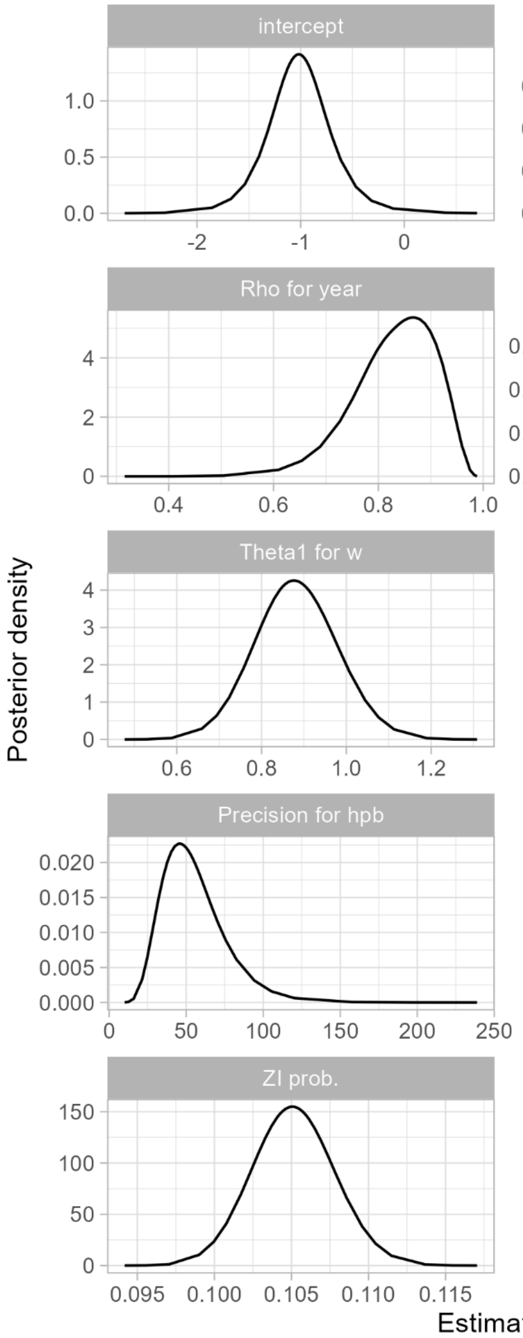


**Fig. 12. Northeast.** Posterior marginal distribution of the fixed effect (intercept), precision for random effects, temporal correlation term (Rho), and spatial field parameters (Thetas).

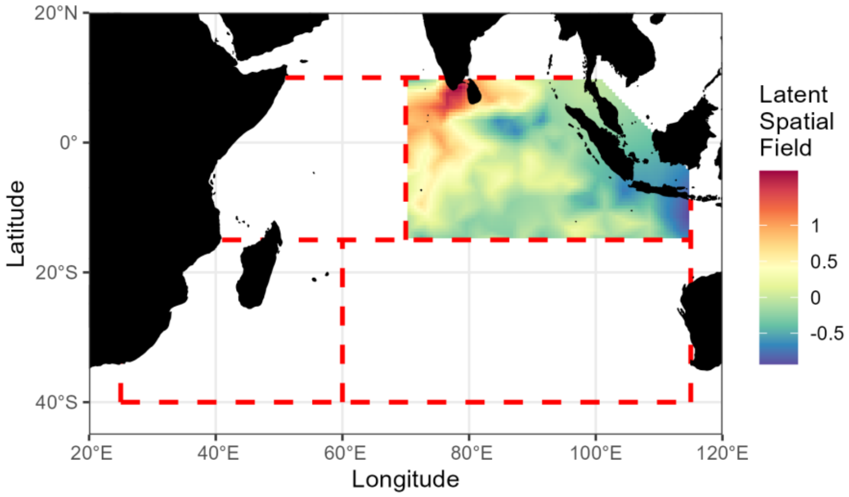


**Fig. 13.** Mean latent spatial field for the northeastern Indian Ocean.

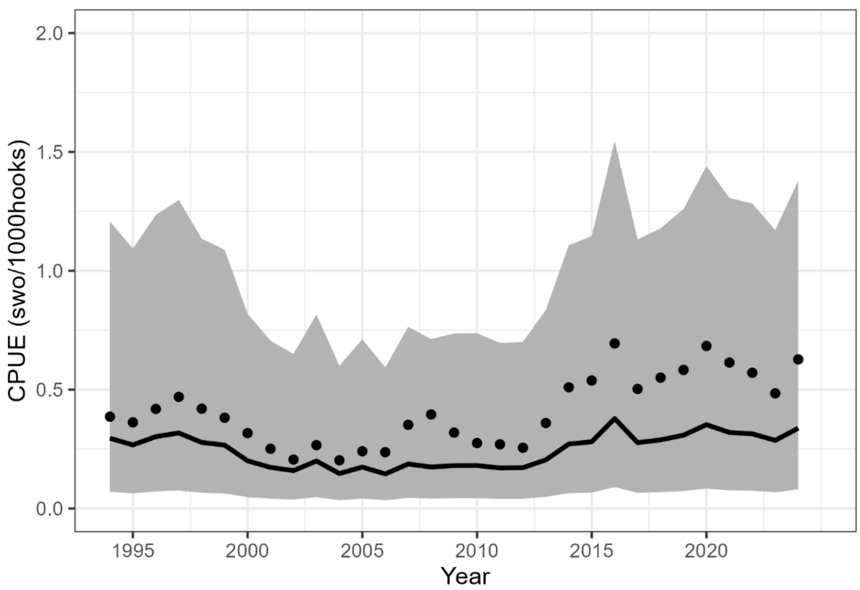


**Fig. 14. Northeastern Indian Ocean.** Historical changes in CPUEs. The solid line represents the standardized CPUE and shaded area indicates the 95% credible interval. Points denote nominal CPUE.

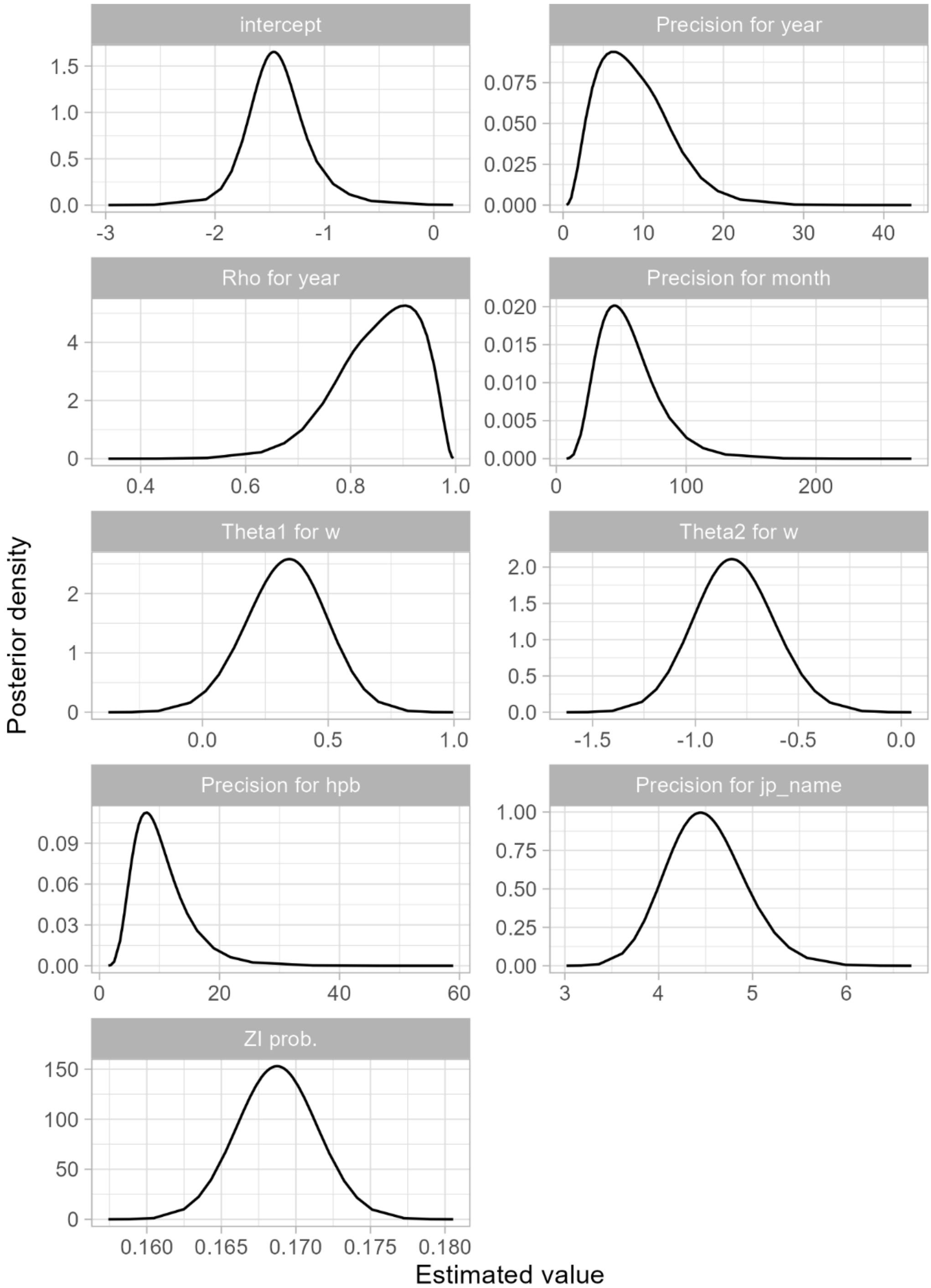


**Fig. 15. Southwest.** Posterior marginal distribution of the fixed effect (intercept), precision for random effects, temporal correlation term (Rho), and spatial field parameters (Thetas).

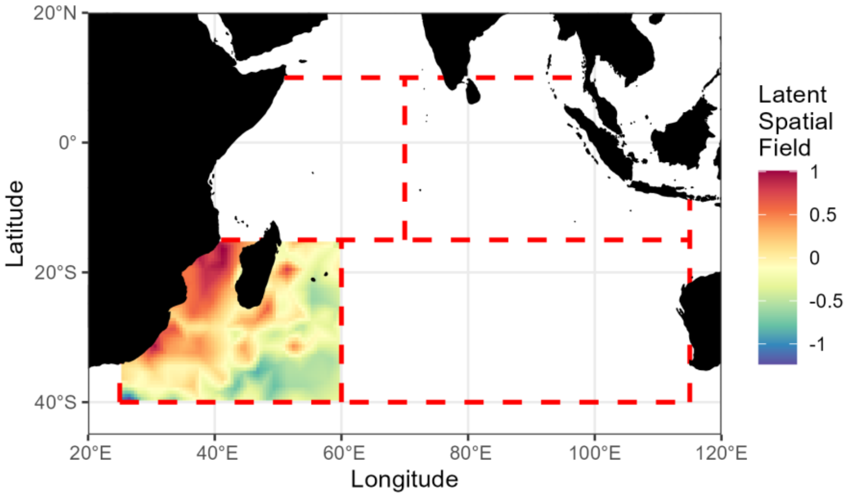


**Fig. 16.** Mean latent spatial field for the southwestern Indian Ocean.

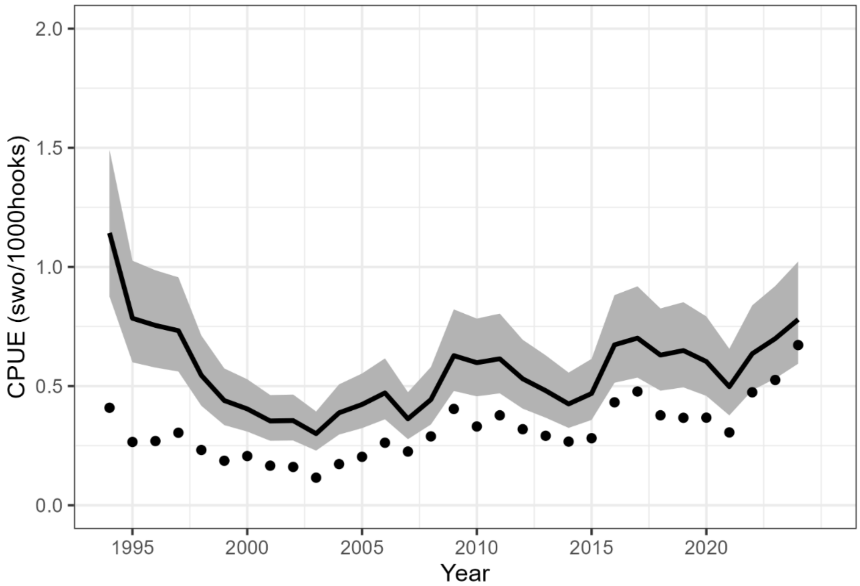


**Fig. 17. Southwestern Indian Ocean.** Historical changes in CPUEs. The solod line represents the standardized CPUE, and the shaded area indicates the 95% credible interval. Points denote nominal CPUE.

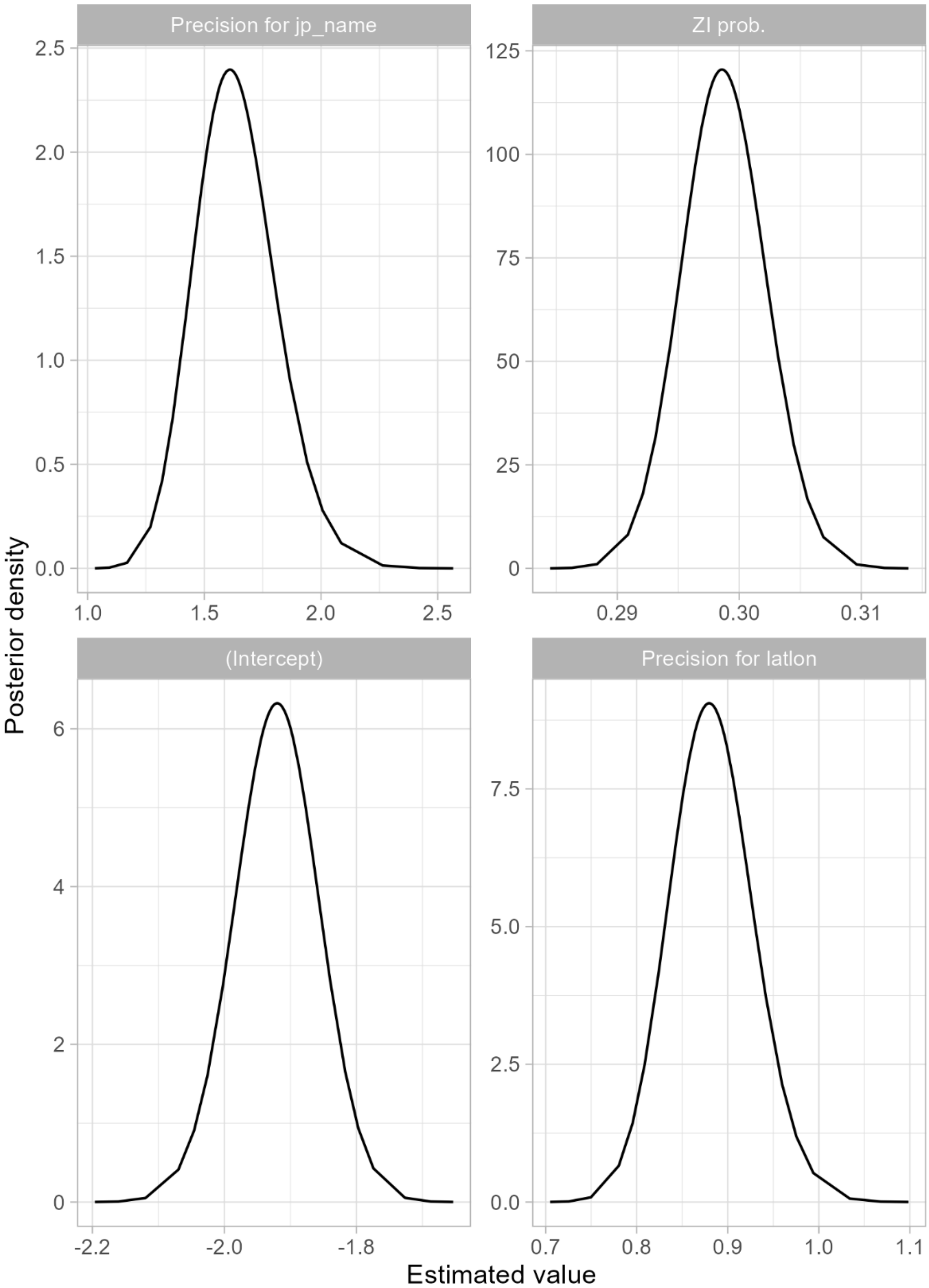


**Fig. 18. Southeast.** Posterior marginal distribution of the fixed effect (intercept), and random effect precision. Note that non-spatial, non-autoregressive model (m_zip_glmm) was used for the period 1994-2024.

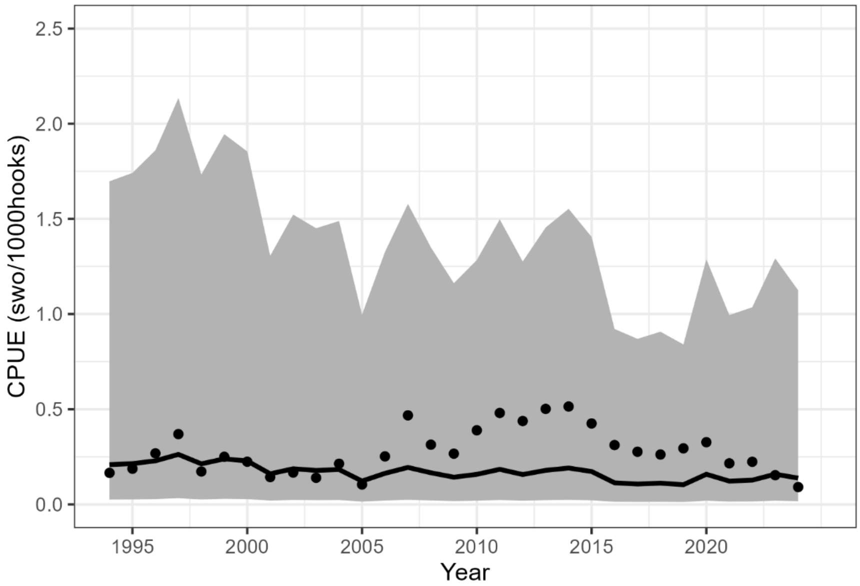


**Fig. 19. Southeastern Indian Ocean.** Historical changes in CPUEs. The solid line represents the standardized CPUE, and the shaded area indicates the 95% credible interval. Points denote nominal CPUE.

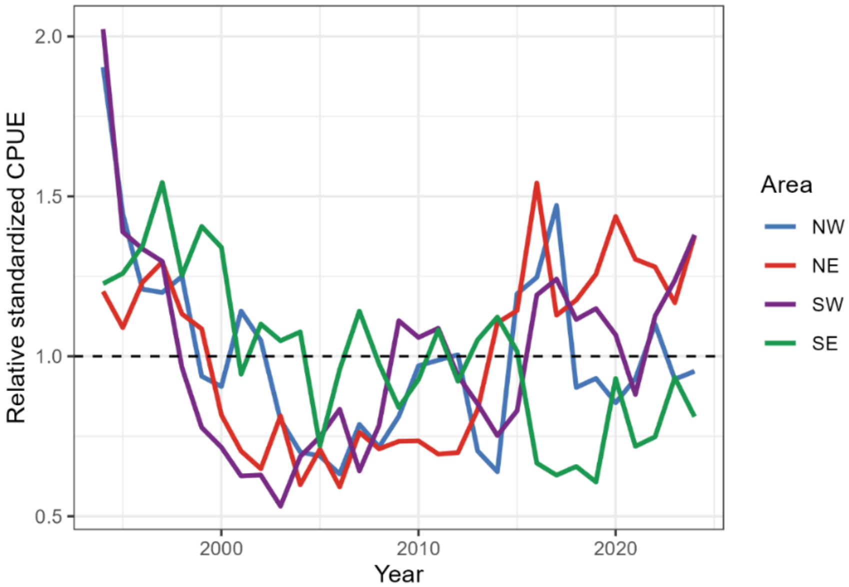


**Fig. 20.** Comparison of relative standardized CPUEs of swordfish caught by the Japanese longline fisheries among the four areas in the Indian Ocean.

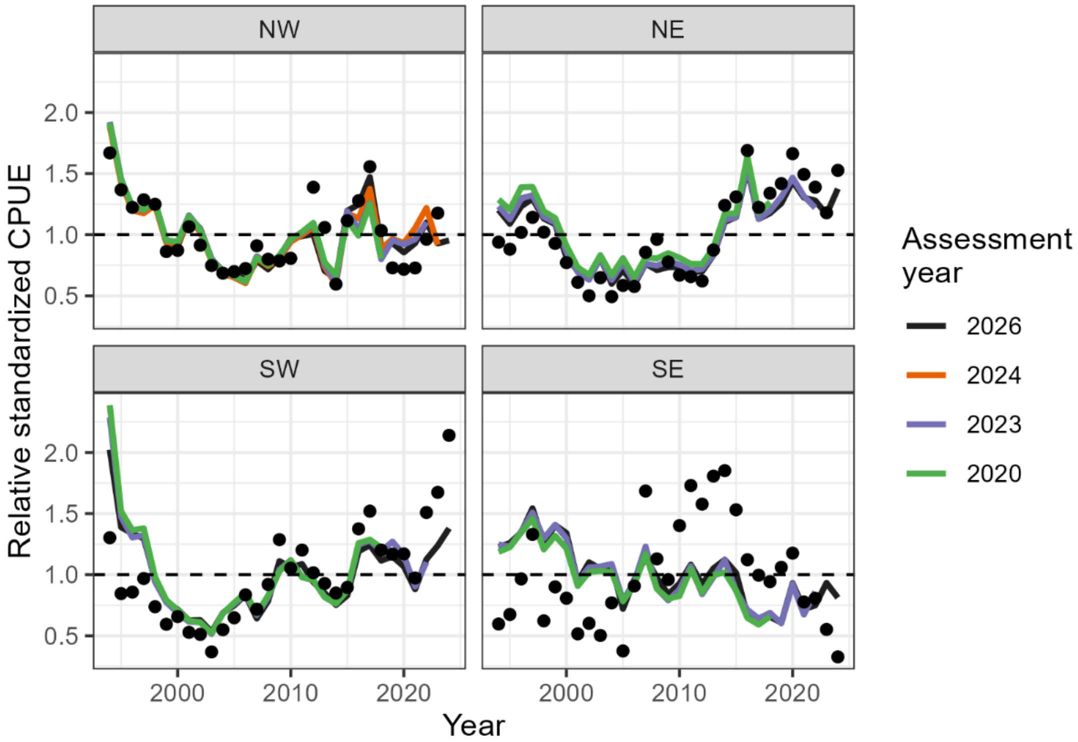


**Fig. 21.** Comparison of relative standardized swordfish CPUE among the four areas in the Indian Ocean during 1994-2024. Estimates from present study (2026) are shown in black solid lines, those from Taki et al. (2020) by green solid lines, those from Matsumoto et al. (2023) by purple solid lines, and those from IOTC (2024), which were used in the 2024 MSE input, by red solid lines. Black filled circles indicate nominal CPUE.